CHAPTER 3

THE NOTCH-TOUGHNESS OF WELDED 14% CHROMIUM STEELS

SYNOPSIS

A new bead-on-plate bend test has been developed to measure the toughness of the narrow (0.25 - 0.35 mm), coarse grained, high temperature heat affected zone (HT HAZ), adjacent to the fusion line, in bead-on-plate welds on 6 mm hot rolled 14 percent chromium steel plate. The test is applied to study the influence of factors like stabilising elements (titanium vs. vanadium), phase composition of the HT HAZ, punch speed during bend testing and weld metal mechanical properties, on the fusion line notch fracture toughness of welds. The fracture toughness is characterised by a fracture appearance transition temperature (FATT).

The FATT temperature of the HT HAZ of steels with less than 60 percent ferrite in the HT HAZ increased at decreasing punch speeds below 133 mm/min. (during bend testing) and higher weld metal strength values. The HT HAZ FATT temperatures of two titanium stabilised steels with respectively 69 and 79 percent ferrite in the HT HAZ are respectively 67 and 74°C for slow bend testing. The HT HAZ FATT temperatures of both titanium and vanadium stabilised steels with less than 60 percent ferrite in the HT HAZ are higher than the reported values. This is due to the fact that the fusion line notch-toughness is enhanced by the ductile properties of the austenitic weld metal. The experimental results are explained in terms of Cottrell's and Davidenkov's fracture theories and the relative strain rate sensitivities of the yield and fracture strength of the austenitic weld metal and ferritic HT HAZ.

Large fractions, low carbon (< 0.028%), titanium stabilised martensite has not resulted in a significant improvement of the fracture toughness of the HT HAZ of welds on 6 mm hot rolled 14 percent chromium steel plate. It is suggested that the fracture toughness is determined by another important factor or phenomenon which has not yet been identified in this study so far.

THE NOTCH-TOUGHNESS OF WELDED 14% CHROMIUM STEELS

1. INTRODUCTION

3CR12 was developed as a replacement for mild and low alloy steels for application in mildly corrosive environments. In order to make provision for applications where more severe corrosive environments are encountered, attention was given to the development of a duplex ferrite-martensite stainless steel with a higher chromium and nickel content (3CR14), using the same principles employed in the development of 3CR12. Although a provisional patent has been lodged recently, the 14% chromium steels are currently not being produced commercially.

As far as the weldability of 3CR12 is concerned, the possibility of the fracture toughness of the narrow HT HAZ being much lower than anticipated, even at high low carbon martensite contents, has already been pointed out in chapter 1. A similar narrow coarse grained HT HAZ develops in welds of the 14% chromium steels. In fact the microstructure and phase composition of the weld HAZ (fig. 3.1) are very similar to that of 3CR12. The development of the microstructures of the different zones in the HAZ therefore may also be similary explained using the pseudo-binary phase diagram for 14% chromium steels(14). This particular study is therefore mainly concerned with the measurement of the fracture toughness of the HT HAZ, adjacent to the fusion line, of bead-on-plate welds on 6 mm plate. The contribution of this narrow HT zone to the notch-toughness of welds on 14% chromium steels has not been quantified as yet.

This HT HAZ appears to have no significant effect on the plane stress toughness of welds on 3CR12 and 14% chromium steels. Slow bend tests, with the weld root in tension and compression respectively, were performed in this study on welds made from tempered 6 mm plate and 180°C bends were successfully achieved. Satisfactory results were also obtained from crossweld tensile tests with fracture occurring in the low temperature HAZ. However, the HT HAZ may have a significant influence on the notch-toughness of welds in critical applications where plane strain conditions rather than plane stress conditions are approached. Brittle fracture may occur in this zone when subjected to a triaxial stress state due to the presence of fusion line defects or in weld configurations offering a high degree of

constraint.

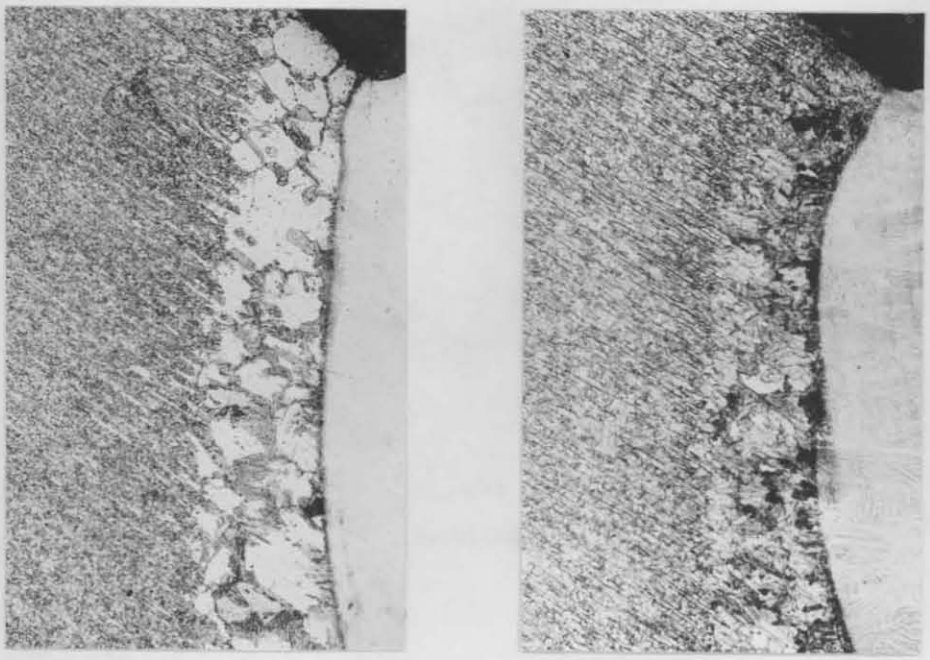

a. b.

Figure 3.1: Weld HAZ microstructure of bead-on-plate welds on hot rolled 6 mm 14% chromium steels.

a. 69% ferrite and 31% grain boundary martensite in the HT HAZ (80x).

b. 96% martensite in HT HAZ. Note the coarse microstructure of the HT HAZ relative to that of the rest of the HAZ even at such a high martensite content (80X).

The limitations of the Charpy impact and CTOD tests for measuring the fracture toughness of the narrow HT HAZ, in especially welded 6 mm plate, have already been dealt with in the first chapter. In theory the toughness of the HT HAZ can be studied by subjecting full Charpy specimens to the same thermal cycle. For this purpose the thermal cycle of this zone, during welding, can be determined experimentally and subsequently simulated in full or sub-size Charpy specimens, in order to produce a large specimen with a phase composition and structure similar to the coarse grained HAZ. This technique has certain important limitations. It is, for example,

difficult to obtain accurate measurements of the thermal cycle of the coarse grained HAZ, which is virtually heated to the solidus temperature. Furthermore, the maximum temperature as well as the subsequent fast cooling rate which are important variables, would be practically impossible to produce experimentally, if the phenomenon of high-temperature embrittlement of the ferrite phase, due to oversaturation with carbon and nitrogen, is considered(3). It is also doubtful whether it is possible to simulate the very fast cooling cycle even in a sub-size Charpy impact specimen and produce a specimen with a homogeneous microstructure and phase composition. Thomas and Apps found that it is generally impossible to match both grain size and hardness to actual weld HAZ structures(7). Even if it was possible to simulate the microstructure in a Charpy impact specimen, the measured toughness is still questionable due to the absence of the constraint associated with the adjacent weld and base metal. It will be shown in this study that the fracture behaviour of the narrow HT HAZ of actual welds is strongly dependent on the cumulative effect of the adjacent weld metal and fine grained HAZ which have totally different mechanical properties and fracture characteristics.

The fusion line fracture behaviour of welds on 14% chromium steel plate was investigated in the present study with particular reference to the following aspects:

a. The development of a new test method for measuring the fracture toughness of the HT HAZ of bead-on-plate welds on 6 mm plate.

b. The influence of factors like phase composition, weld metal mechanical properties and loading rate on the fracture response of the HT HAZ.

c. The relative effects of respectively titanium and vanadium on the fracture toughness of the HT HAZ. The possibility of substituting some of the titanium, which is commonly used as a stabilising element, with vanadium.

d. Interpretation of experimental results with flow stress-fracture stress theories.

2. EXPERIMENTAL PROCEDURE

2.1 Notch-toughness testing

During the past 30 years various tests have been developed to evaluate the brittle fracture characteristics of welds. Almost all of those tests involve the introduction of a notch and the determination of the ductile to brittle transition temperature. Although each test emphasizes a different feature of the brittle-fracture process, none was found suitable to evaluate the influence of this narrow coarse grained HAZ on the notch-toughness of welds on 6 mm 14% chromium steel plate. Among the various tests proposed, the Charpy test is the most widely used. (The limitations of this test for application to welds on 6 mm plate have already been dealt with in chapter 2).

After various attempts to develop a test method which will yield information on the effect of the HT HAZ on the fracture behaviour of actual welds, the test specimen shown in figure 3.2 was developed. It is a bead-on-plate welded specimen (6 mm x 10 mm x 58 mm) which was machined from 6 mm hot rolled plate on which a single bead was welded perpendicular to the rolling direction. The process variables were designed especially to obtain the excessive large welding bead together with the deep penetration with a fusion line which will ideally be oriented normal to the plate surface (fig. 3.3). Single beads were welded according to the following welding procedure:

Welding process	:	Gas metal-arc (MIG)
Welding wire	:	AISI 316L (1.6 mm dia.)
Shielding gas	:	84% Ar, 13% CO_2 , 3% O_2
Welding position	:	Flat
Current	:	360-380 amps.
Volts	:	20-22
Arc speed	:	93-95 cm/min.
Heat input	:	0.46-0.52 kJ/mm

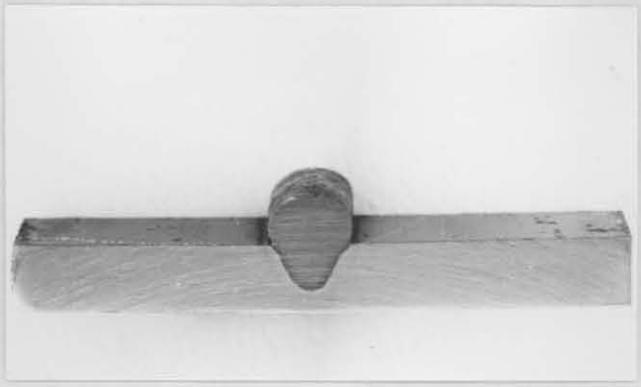

Figure 3.2: Bead-on-plate welded fusion line fracture toughness test specimen (6 mm x 10 mm x 55 mm).

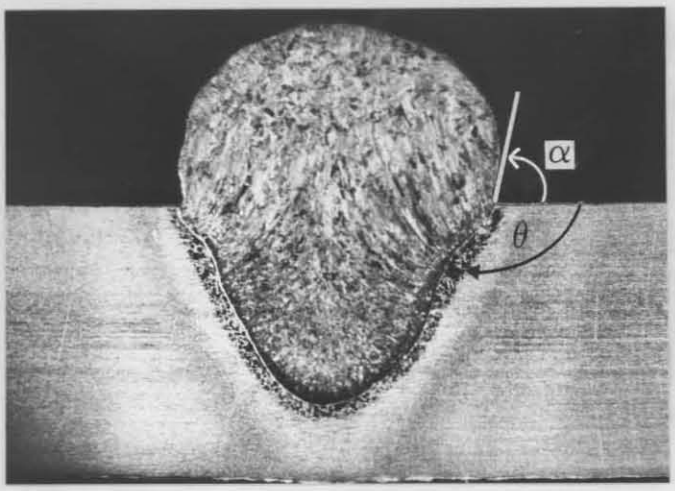

Figure 3.3: Weld bead details of bead-on-plate welded test specimen. Note the coarse grained HT HAZ adjacent to the fusion line.

Some of the details of the weld bead in figure 3.3 are as follows:

Penetration	:	60-65%
Dilution with base metal	:	40-45%
Fusion line orientation (θ)	:	119 - 125° (fig. 3.3)
Included angle (α) between weld bead and plate surface	:	58-62° (fig. 3.3)
Width of HT HAZ	:	0.2-0.3 mm

The welded bead-on-plate test specimens were tested by three-point face-bending at different temperatures to obtain a fusion line fracture appearance transition temperature (FATT). Bend testing was executed at a

punch speed of 133 mm/min., using an anvil with a radius equal to plate thickness. The weld bead which is subjected to tensile bending stresses is located with a transverse orientation in the centre of the bend test specimen.

The tip of the natural notch or stress concentration, which is created by the large welding bead, is located on the fusion line (fig. 3.4). The notch tip radius range from 0.15 mm to 0.25 mm. A triaxial stress field developes during bending at the notch tip due to the constraint produced by the large welding bead and the high strength of the hot rolled base metal. With the development of a triaxial stress field in both the weld metal and fine grained HAZ adjacent to the coarse grained HAZ at the notch tip, the cumulative effect of the fine grained HAZ, coarse grained HT HAZ, and the weld metal, on the fusion line notch fracture initiation and propagation behaviour may be studied.

Fracture of the 14% chromium steel specimens was found to occur only in the HT HAZ and/or weld metal adjacent to the fusion line. The FATT temperature was determined at 50% ductile (microvoid coalesence) fracture surface. The percentage of the fracture surface which failed in a ductile fashion was determined by area analysis of only that part of the fracture surface where the crack propagated in the HT HAZ and/or weld metal adjacent to the fusion line. Partially cracked as well as fractured specimens were also investigated by optical and scanning electron microscope (SEM) analysis in order to determine the crack path.

Figure 3.4: Notch tip on fusion line of bead-on-plate bend specimen. The tip radius ranged from 0.15 mm to 0.25 mm.

Although the test results of this new test method are dependent on such variables as the size of the HT HAZ (heat input), orientation of the fusion line relative to the plate surface, the base metal strength, loading rate and weld metal properties, an indication can be obtained of the performance of actual welds on 14% chromium steels during very severe loading conditions, where a high degree of constraint prevails. The effect of the fusion line orientation on the test results was kept constant by careful selection of only those specimens with fusion line orientations within the specified range.

2.2 Steel compositions and microstructures

Five titanium stabilised and six vanadium stabilised 14% chromium steels were designed in order to obtain different ferrite and martensite contents in the coarse grained HT HAZ. The steels were designed using Kaltenhauser's relation to obtain a large range of ferrite factors(1). (The ferrite factor is a measure of the relative amounts of ferrite and austenite stabilising alloying elements in stainless steel.) The chemical analysis (wt-%) of the experimental steels are shown in table 3.1. The steels were melted in a laboratory induction furnace in an inert gas atmosfere, cast into 5kg ingots and hot rolled into 6 mm thick plate.

Bead-on-plate welded bend test specimens were prepared from the hot rolled plate with a dual phase microstructure which consists of alternatively pancake shaped ferrite and martensite grains. During bending the HT HAZ is subjected to a larger constraint (higher triaxiality) by the relatively high strength hot rolled plate compared to a lower strength hot rolled-and-tempered plate. The microstructure of hot rolled-and-tempered plate consists of recrystallised ferrite and tempered martensite grains.

The ferrite contents of the HT HAZ of bead-on-plate welds on hot rolled 6 mm plate, of the experimental titanium and vanadium stabilised steels, ranged respectively from 4-79% and 17-55% ferrite. The phase composition of the HT HAZ was determined by area analysis on high contrast photographs prepared at a magnification of 150 times (table 3.1).

Table 3.1: Chemical analysis (wt-%) of experimental 14% chromium steels. The hardness (Vickers) of the hot rolled base metal is also indicated.

Steel	C	N	Mn	Cr	Ni	Si	Ti	V	F.F.*	Base metal hardness, HV
A	0.022	0.026	1.06	13.33	2.88	0.36	0.25	-	1.93	335
B	0.026	0.023	1.01	13,53	2.75	0.42	0.20	-	2.67	354
C	0.028	0.025	1.04	13.47	2.58	0.42	0.24	-	3.39	322
D	0.022	0.026	0.90	13.86	2.64	0.41	0.28	-	4.28	327
E	0.024	0.028	0.94	13.87	2.21	0.37	0.32	-	5.85	315
F	0.024	0.026	0.92	13.63	2.36	0.31	-	0.22	3.31	368
G	0.020	0.026	0.93	13.80	2.39	0.31	-	0.34	4.10	363
H	0.021	0.029	0.96	13.88	2.38	0.34	-	0.36	4.68	373
I	0.021	0.026	1.03	13.61	2.10	0.42	-	0.36	5.59	346
J	0.021	0.023	1.00	13.82	2.11	0.48	-	0.37	6.35	345
K	0.025	0.025	0.74	13.99	1.97	0.48	-	0.33	7.16	357

* Ferrite factor according to Kaltenhauser's (1) equation.

$$F.F. = -40\,(C+N) - 2Mn - 4Ni + Cr + 6Si + 8Ti + 2Al + 4Mo + 5V^{x}$$

x A factor of five was assumed for vanadium.

3. EXPERIMENTAL RESULTS AND DISCUSSION

3.1 Fracture behaviour of titanium stabilised steels with respectively 69 and 79% ferrite in the HT HAZ

The two welded titanium stabilised steels with respectively 69% and 79% ferrite in the HT HAZ fractured in a similar manner. Both cleavage and ductile fractures, which occurred respectively at temperatures below and above the FATT temperature, were confined to the HT HAZ. The other three titanium and all the vanadium stabilised steel specimens which contained less than 60% ferrite in the HT HAZ fractured in a different manner.

The fracture surfaces of specimens of steel D with 69% percent ferrite in the HT HAZ together with the FATT curve are shown in figure 3.5. The

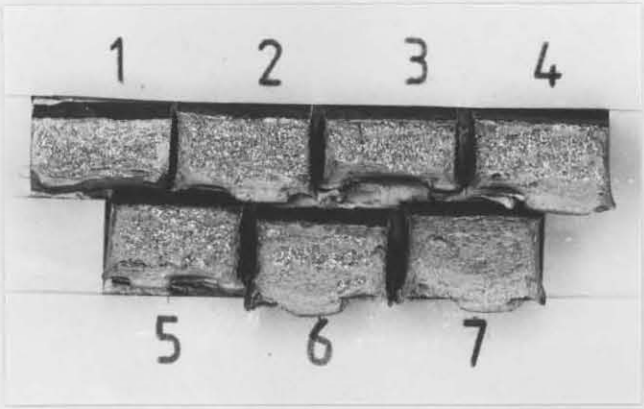

a.

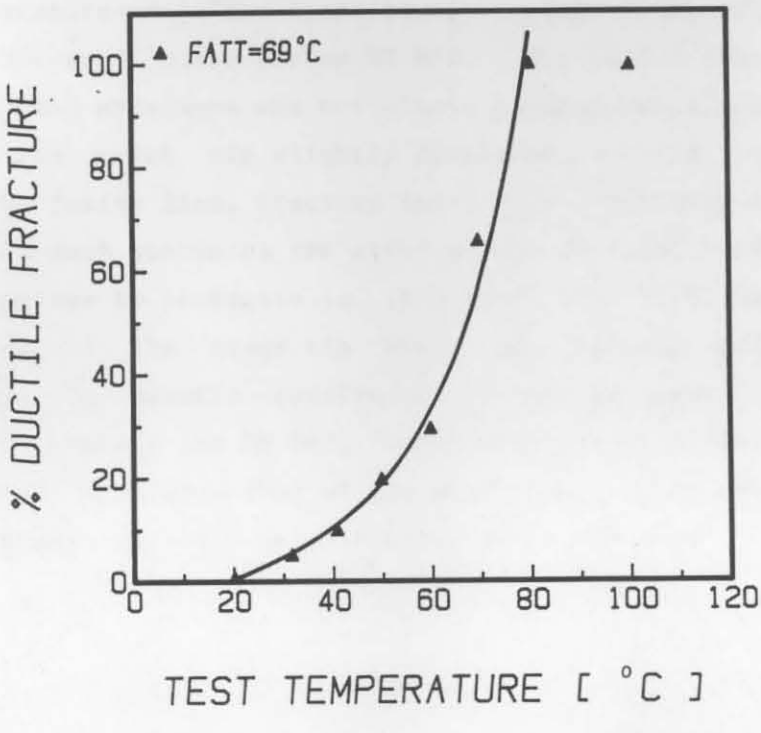

b.

Figure 3.5: a. Fracture surfaces of bead-on-plate bend specimens of steel D with 69% ferrite in the HT HAZ; tested at 1:20°C, 2:30°C, 3:40°C, 4:50°C, 6:70°C and 7:80°C.

b. Fracture appearance transition curve for the HT HAZ of steel D.

fracture path was established on partially cracked specimens. Figure 3.6 shows the crack path of specimens of steel E, with 79% ferrite in the HAZ,

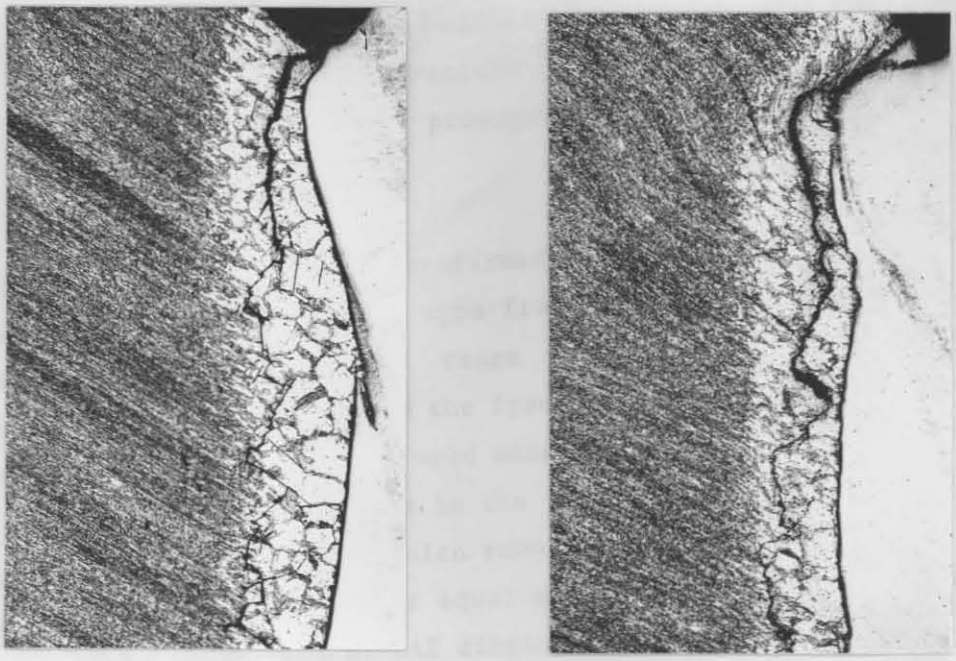

a. b.

Figure 3.6: Cleavage and ductile cracks in the HT HAZ of partially cracked bead-on-plate bend specimens of steel E, with 79% ferrite in the HT HAZ; tested respectively at 20°C (a) and 90°C (b). Magnification 35X. (The deformation which is evident in the specimen tested at 90°C occurred during reverse bending in order to close the ductile crack before polishing).

which were tested at temperatures below (20°C) and above (90°C) the FATT temperature of 74°C, respectively. Both fracture initiation and propagation occurred in the narrow HT HAZ. The fusion line notch tip of some of the bend specimens was not always located exactly on the fusion line. With the notch tip slightly displaced towards the weld metal adjacent to the fusion line, fracture initiation inevitably occurred in the weld metal. In such specimens the crack always deviated immediately to the HT HAZ to continue to propagate in this zone (fig. 3.7). Depending on the distance ahead of the crack tip where the maximum principal stress developes, due to plastic constraint, it can be argued that fracture initiation may occur in the HT HAZ, especially with the fracture stress of the HT HAZ much lower than that of the weld metal, with subsequent crack propagation through the weld metal towards the notch tip.

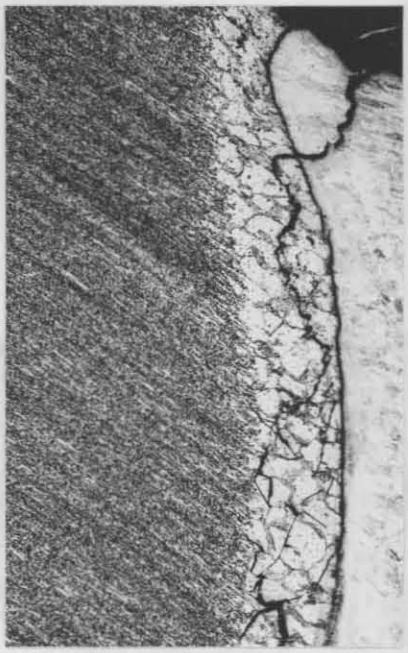

Figure 3.7: Partially cracked bead-on-plate bend specimen of steel D showing ductile fracture initiation in the weld metal and cleavage fracture propagation in the HT HAZ. Specimen tested at 90°C (35X).

The fracture path was also confirmed by SEM analysis of the fracture surfaces. Brittle cleavage type fractures occurred only in the HT HAZ within the test temperature range 0°C to 100°C. Certain distinct differences were observed in the fracture surface appearance of ductile fractures in respectively the weld metal, the coarse grained HT HAZ and the fine grained HAZ. The dimples in the fracture surface of respectively the weld metal and HT HAZ, which resulted from a micro-void coalesence mechanism, are nearly all of equal size, but the weld metal dimples are much smaller than the HT HAZ dimples (fig. 3.8). The ductile fracture surface which resulted from a ductile fracture in the fine grained, low temperature HAZ (the crack left the HT HAZ at the toe of the bead-on-plate weld), contains, however, a combination of relatively small and large dimples (fig. 3.9). It was therefore relatively easy to establish the fracture path by SEM analysis.

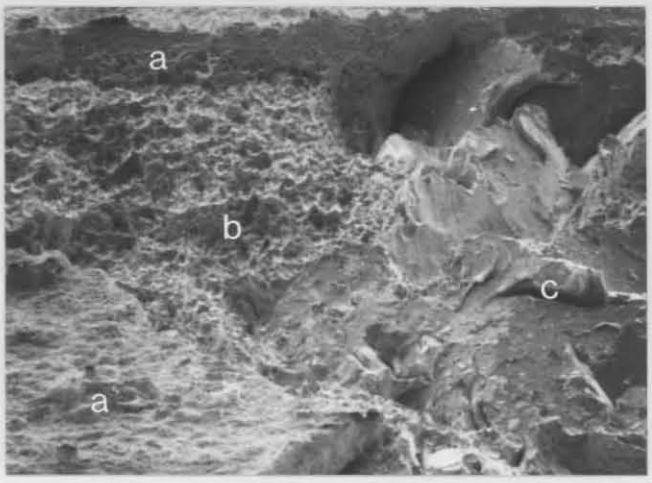

Figure 3.8: SEM fracture surface appearance of a bead-on-plate bent specimen; note ductile fracture in the weld metal (a) adjacent to the fusion line, ductile fracture in the HT HAZ (b) and cleavage fracture in the HT HAZ (c). The large cleavage facets resulted from the large grain size of the HT HAZ (100X).

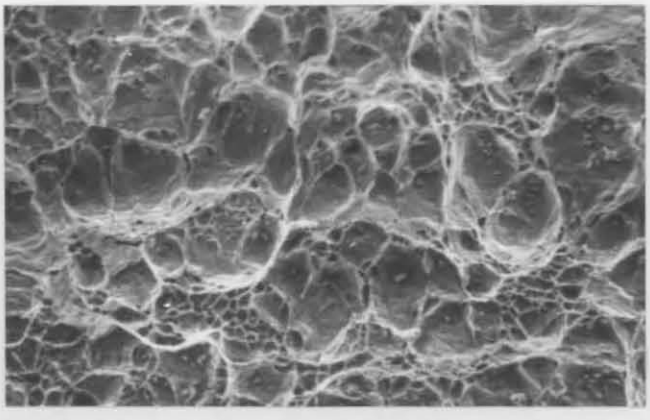

Figure 3.9: SEM fracture surface of a ductile fracture in the fine grained low temperature HAZ (825X).

3.2 Fracture behaviour of titanium and vanadium stabilised steels with less than 60% ferrite in the HT HAZ.

The three titanium and five vanadium stabilised steel bead-on-plate bend specimens with less than 60% ferrite in the HT HAZ fractured in a manner different from the titanium stabilised specimens with more than 60% ferrite in the HT HAZ. Brittle cleavage fracture at temperatures below the FATT and ductile fracture at temperatures above the FATT was confined respectively to the HT HAZ and weld metal adjacent to the fusion line (fig. 3.10). At the FATT temperature a ductile crack initiated in the weld metal and propagated for a certain distance in the weld metal, at a distance of 0.2 to 0.3 mm from the fusion line, before it deviated into the coarse grained HT HAZ to propagate further in a cleavage mode (fig. 3.11).

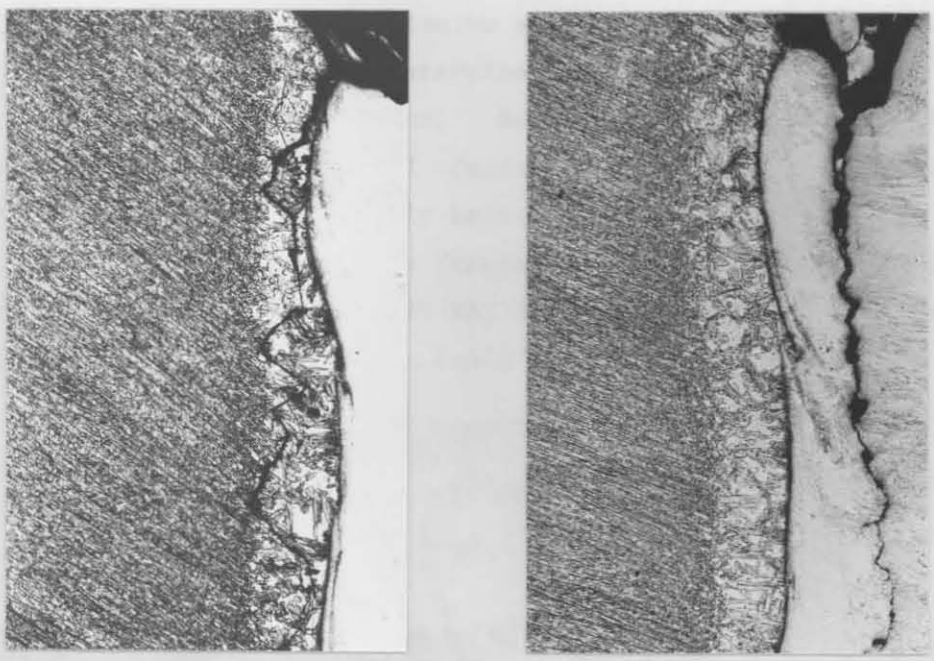

a. b.

Figure 3.10: Crack paths in partially fractured specimens of steel F with 17% ferrite in the HT HAZ (35X).
a. Brittle cleavage fracture in HT HAZ of a specimen tested at 5°C
b. Ductile fracture in weld metal of a specimen tested at 30°C

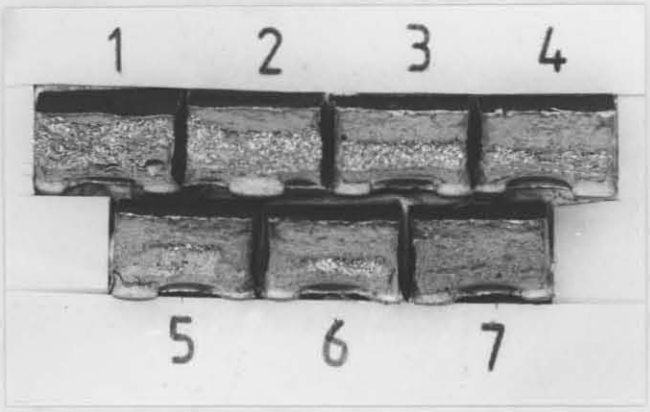

Figure 3.11: Fracture surfaces of bead-on-plate bend specimens of steel G with 24% ferrite in the HT HAZ, tested at: 1:10°C, 2:20°C, 3:32°C, 4:42°C, 5:52°C, 6:62°C and 7:72°C. The dull fracture surface resulted from ductile fracture in the weld metal while the bright fracture surface resulted from brittle cleavage fracture in the HT HAZ.

The phase composition and FATT values of the HT HAZ of the experimental steels in table 3.1 is summarized in table 3.2 and figure 3.12. A relationship was developed to calculate the amount of ferrite contained in the HT HAZ adjacent to the fusion line. The following equation was developed by multilinear regression analysis using the data in tables 3.1 and 3.2.

$$\%\ \text{ferrite in HT HAZ} = -798(\%C) + 4000(\%N) + 32(\%Mn) + 78(\%Cr) - 82(\%Ni) + 184(\%Si) - 180(\%Ti) - 320(\%V) - 777.$$

The FATT of the HT HAZ of the titanium stabilised steels with 69% and 79% ferrite in the HT HAZ, has been determined, since both brittle and cleavage fractures were limited to this zone. However, the FATT of the HT HAZ of the steels with less than 60% ferrite in this zone has not been determined, due to the completely brittle behaviour of this zone at the FATT temperature where 50% ductile fracture was confined exclusively to the weld metal. The FATT of the HT HAZ of these steels will therefore be higher than the values reported in table 3.2 and figure 3.12.

Table 3.2: Phase composition and FATT temperatures of the HT HAZ of bead-on-plate welds on 6 mm hot rolled plate of the steels in table 3.1.

Titanium stabilised 14% chromium steels

	Steel A	Steel B	Steel C	Steel D	Steel E
% Ferrite in HT HAZ	3.5	4	19	69	79
FATT (°C)	20	13	26	67*	74*

*Both ductile and brittle fractures occurred in the HT HAZ while ductile fracture occurred for all the other steels exclusively in the weld metal.

Vanadium stabilised 14% chromium steels

	Steel F	Steel G	Steel H	Steel I	Steel J	Steel K
% Ferrite in HT HAZ	17	24	32	44	48	55
FATT (°C)	13	39	37	40	56	60

Figure 3.12 shows a decrease in the FATT of the HT HAZ of both titanium and vanadium stabilised steels with a decrease in ferrite content. However, it is not possible at this stage to come to any conclusions as far as the relative effects of titanium and vanadium on the toughness of the HT HAZ are since the FATT of the HT HAZ of most of the steels have not yet been determined. The FATT values of the HT HAZ of the vanadium steels are expected to be higher than that of the titanium steels due to the lower stability of the vanadium carbonitrides and therefore higher total dissolved carbon and nitrogen contents.

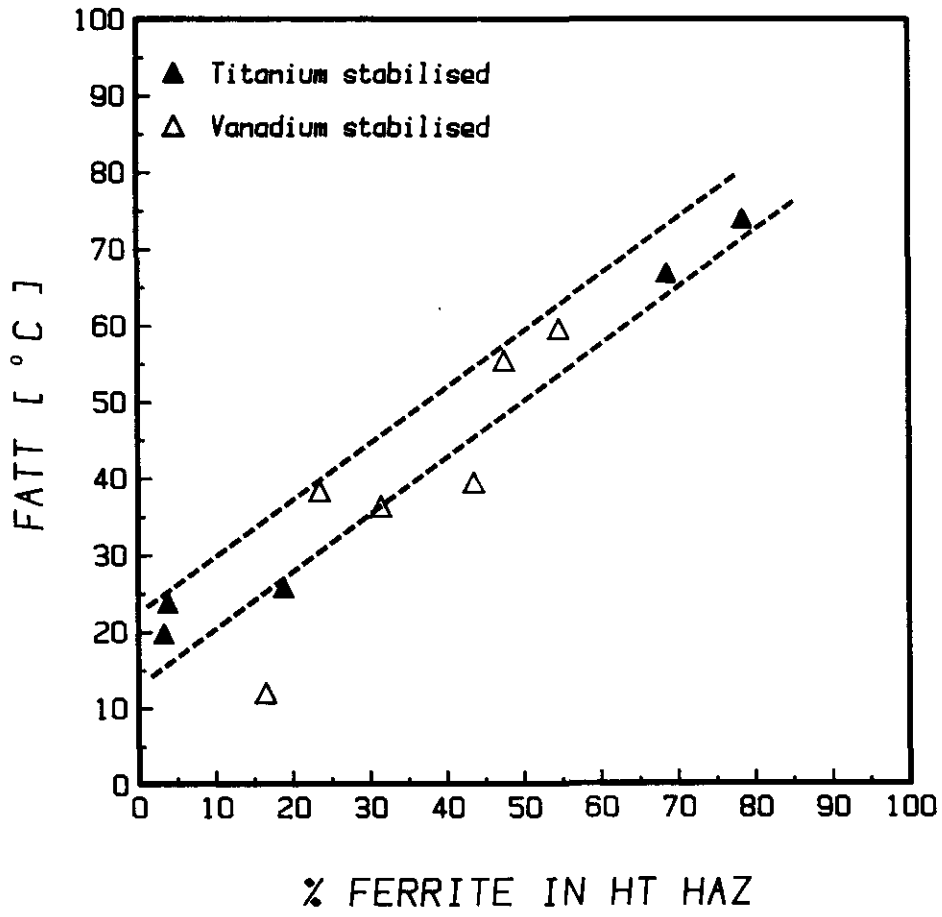

Figure 3.12: FATT temperature versus phase composition of the coarse grained HT HAZ of 14% chromium steels, stabilised respectively with titanium and vanadium.

3.3 The effect of loading rate and weld metal properties on the fusion line fracture behaviour of steels with less than 60% ferrite in the HT HAZ

The FATT temperatures of the HT HAZ of both the vanadium and titanium stabilised steels with less than 60% ferrite in the HT HAZ have not been determined yet since the fusion line fracture toughness, of welds on these steels, are artificially enhanced by the ductile property of the austenitic AISI 316L weld metal. The FATT temperature of the HT HAZ are therefore determined not only by the properties and size of this zone, but also by the mechanical properties and fracture toughness of the weld metal. Furthermore, since the yield strength of body-centered cubic metals (such as the HT HAZ) is far more sensitive to temperature and strain rate

changes, than it is in face-centered cubic metals (such as the austenitic weld metal), it was thought that the FATT temperature of the HT HAZ of steels with less than 60% ferrite in this zone might be sensitive to strain rate changes. This strain rate sensitivity in BCC metals may be related to the temperature-sensitive Peierls-Nabarro stress contribution to the yield strength, which is much larger in BCC metals than in FCC metals.

3.3.1 Loading rate or punch speed

The FATT temperatures in table 3.2 and figure 3.12 were determined at a loading rate or punch speed during bend testing of 133 mm/min. The FATT temperature of the HT HAZ of steel J with 48% ferrite in this zone increased from 56°C to 76°C with a decrease in punch speed from 133 mm/min. to 4 mm/min. (fig. 3.13). The FATT temperature of a homogeneous material is generally not sensitive to loading rate variations within this range. Even at this new FATT temperature of 76°C, the 50% ductile fracture surface resulted from ductile fracture in the weld metal with a completely cleavage fracture in the HT HAZ. The FATT of the HT HAZ is therefore even higher than 76°C.

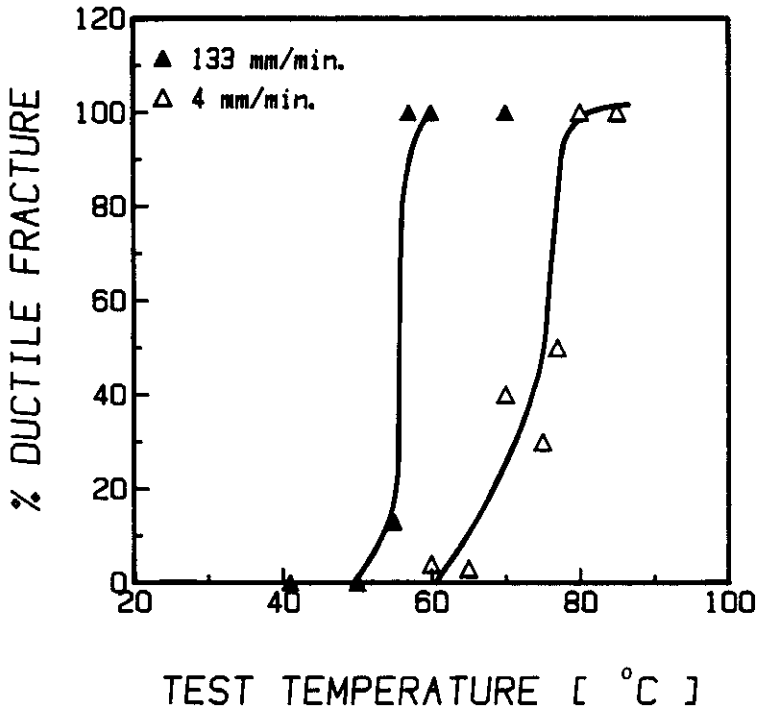

Figure 3.13: Fracture appearance transition curves for steel J with 48% ferrite in the HT HAZ determined at two punch speeds of respectively 133 mm/min. and 4 mm/min..

The FATT temperature of the titanium stabilised steel with 79% ferrite in the HT HAZ, determined at a punch speed of 133 mm/min., is 74°C (table 3.2). With the FATT of the HT HAZ of the vanadium stabilised steel with only 48% ferrite in this zone much higher than 76°C, it is clear that the FATT of this zone of a vanadium stabilised steel, with 79% ferrite in this zone, will be much higher (as expected) than that of a titanium stabilised steel. It may therefore be concluded that the FATT temperature of the HT HAZ of the vanadium stabilised steels will be higher than that of the titanium stabilised steels for any ferrite content in this zone although this is not suggested by the results in figure 3.12.

The effect of punch speed, within the range 2 mm/min. to 240 mm/min., on the FATT temperatures of the HT HAZ of steels A (3CR14Ti), C (3CR14Ti) and J (3CR14V) with respectively 3.5%, 19% and 48% ferrite in the HT HAZ, is summarized in figure 3.14. The FATT temperature were unchanged at punch speeds above about 133 mm/min., but increased considerably at punch speeds below 133 mm/min. The FATT temperatures of specimens tested by impact loading in a Charpy impact machine are very similar to the temperatures obtained in slow, three point bend testing at a punch speed of 133 mm/min. An increase of about 20°C was observed for steels C and J with a decrease in punch speed from 133 mm/min. to 7 mm/min.. These much higher FATT temperatures obtained at such extremely low punch speeds are not yet the true FATT temperatures of the HT HAZ. The HT HAZ still fractured in a completely brittle cleavage manner at the FATT temperature with ductile fracture in the weld metal adjacent to the fusion line.

It may be concluded at this stage that the HT HAZ FATT temperature of 14% chromium steels with less than 60% ferrite in the HT HAZ depends not only on the phase composition of this zone and the fusion line orientation relative to the plate surface but that it also depends on the punch speed during bend testing. The effect of fusion line orientation was controlled by careful selection of those specimens with a fusion line orientation within the specified range of 122 $\pm$ 3 degrees. The FATT of the HT HAZ of steels with more than 60% ferrite in this zone was not effected by the punch speed within the range 2 mm/min. to 400 mm/min.

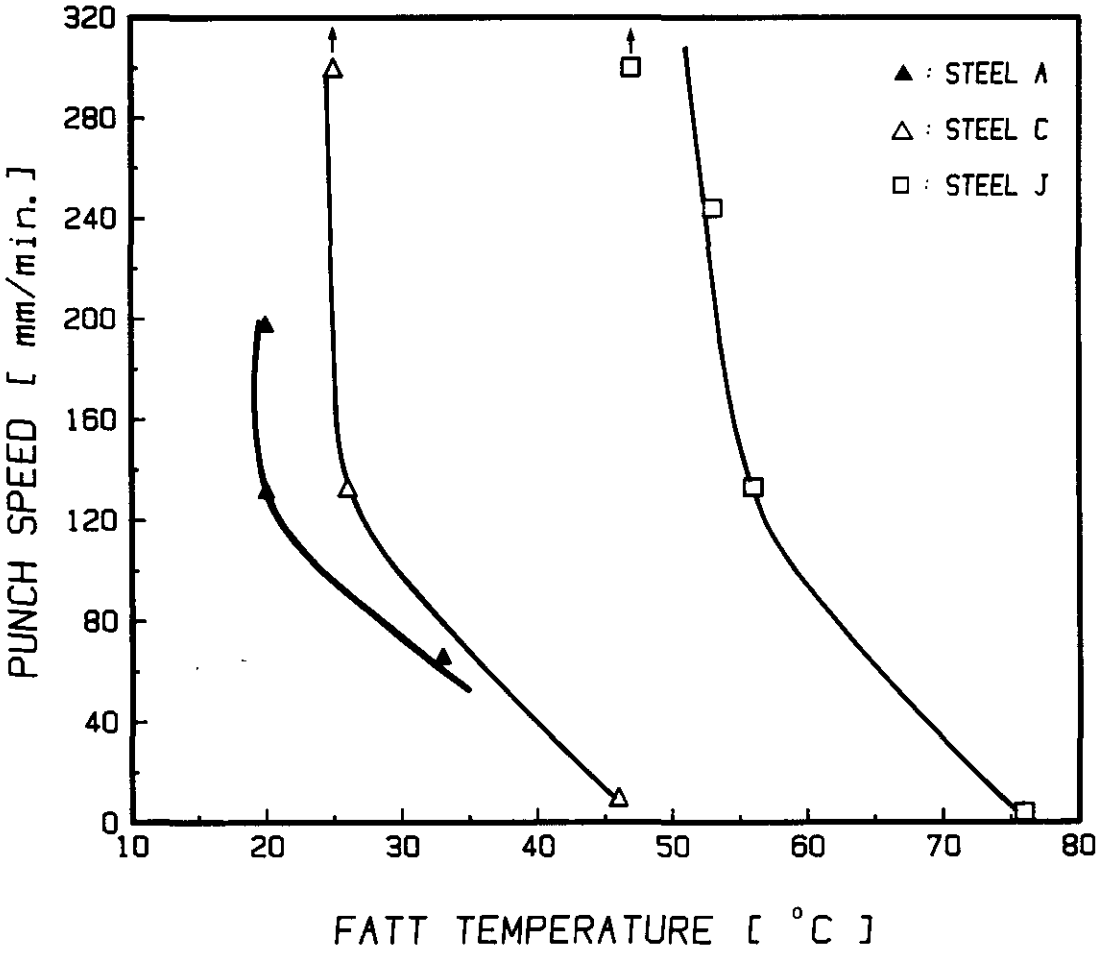

Figure 3.14: Punch speed for bend testing versus the FATT temperature of the HT HAZ of steels A, C and J with respectively 3.5%, 19% and 48% ferrite in the HT HAZ. The FATT temperatures indicated at a punch speed of 300 mm/min. were determined by impact loading of the specimens in a Charpy impact machine.

3.3.2 Weld metal properties

Another important aspect which has not yet been dealt with is the effect of the weld metal mechanical properties, i.e. yield strength, tensile and fracture stress, and the work hardening rate on the FATT of the HT HAZ of welds with less than 60% ferrite in the HT HAZ. According to Davidenkov's flow stress-fracture stress theory, the FATT temperature may be increased by increased weld metal strength properties relative to that of the HT HAZ. With the strength properties of the weld metal, especially the fracture stress (the fracture stress of the weld metal adjacent to the fusion line

is inter alia determined by the degree of constraint or stress triaxiality) much higher than that of the HT HAZ, within the temperature range 0°C to 100°C, it will be possible to determine the true FATT (with both cleavage and brittle fractures confined to the HT HAZ) of the HT HAZ.

The microhardness transverse across the fusion line of bead-on-plate AISI 316L welds on 6 mm hot rolled plate of steels E (3CR14 Ti) and G (3CR14V) with respectively 79% and 24% ferrite in the HT HAZ is shown in figure 3.15. The indicated hardness of the HT HAZ is the weighed average hardness of the martensite and ferrite in the HT HAZ. Both brittle and cleavage

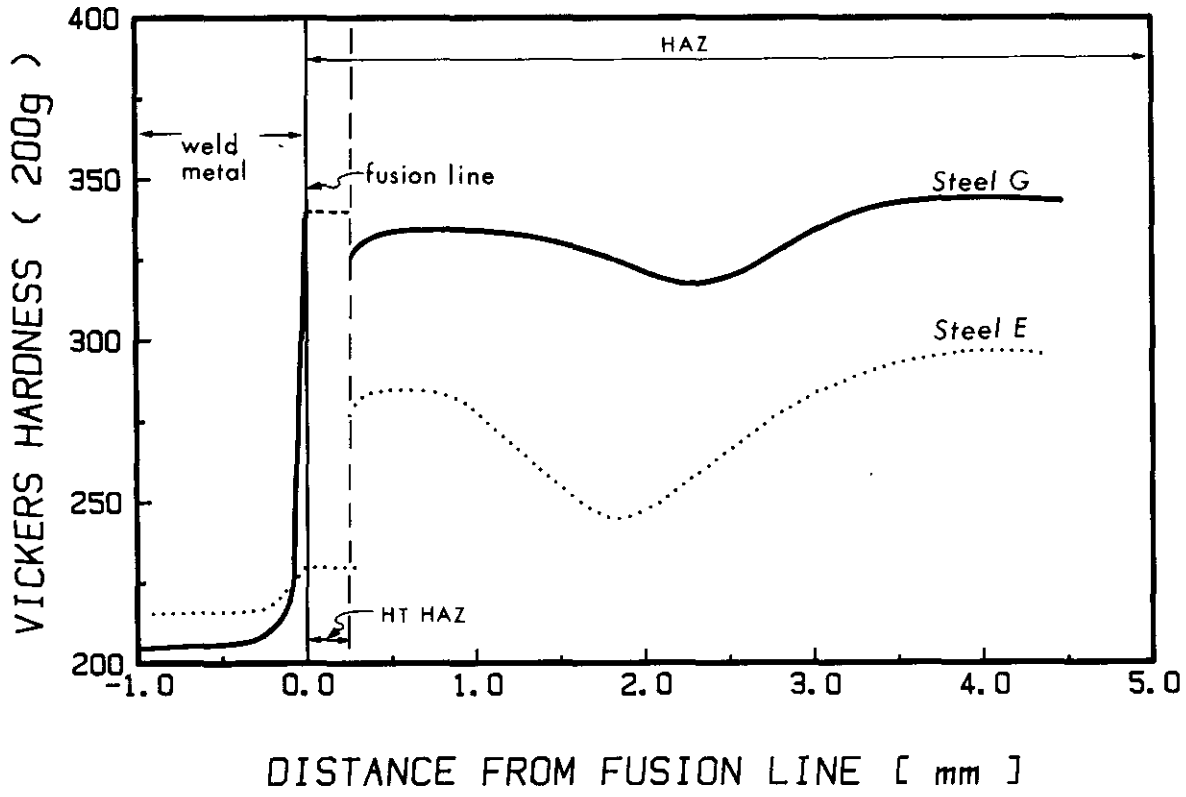

Figure 3.15: Microhardness transverse across the fusion line of bead-on-plate welds on 6 mm hot rolled plate of steel E and G with respectively 79% and 24% ferrite in the HT HAZ.

fractures occurred during bend testing in the HT HAZ of steel E due to the lower fracture stress of this zone compared to that of the adjacent weld metal and fine grained HAZ. The lower fracture stress may be attributed to the much larger grain size (ASTM No 1-2), the high ferrite content and the

higher work hardening rate of the austenitic weld metal. The hardness of this zone is also much lower than that of the adjacent fine grained HAZ and nearly equal to that of the weld metal (fig. 3.15).

At temperatures above the FATT temperatures of the HT HAZ of steels with less than 60% ferrite in this zone, ductile fractures occurred in the weld metal due to the higher fracture stress of the HT HAZ. The hardness of, e.g., the HT HAZ of steel G in figure 3.15 is much higher that that of the weld metal due to the presence of 76% martensite in this zone. The higher fracture stress of the HT HAZ, even with the much higher work hardening rate of the austenitic weld metal may therefore be attributed to the higher tensile strength (which is proportional to the hardness) and finer grain size compared to a zone with 79% ferrite.

In paragraph 3.1 it was specified that the bead-on-plate bend specimens were welded within the heat input range of 0.46 kJ/mm to 0.52 kJ/mm. Most specimens were welded at the lower end of this range. To study the effect of the weld metal mechanical properties on the FATT or fracture behaviour of the HT HAZ, an additional series of specimens of steels B, H and J were prepared by welding at the higher end of the heat input range in order to obtain a slightly higher dilution with the base metal, with improved weld metal strength properties.

The results which are summarized in table 3.3 show that the FATT temperature of the HT HAZ increased with a slight increase in weld metal hardness and therefore fracture stress. Figure 3.16 shows both effects of the weld metal strength and punch speed on the FATT of the HT HAZ of steel B with 96% martensite in this zone. This effect of the weld metal hardness seems to decrease with a decrease of punch speed from 133 mm/min. to 10 mm/min.

Table 3.3: FATT temperatures of the HT HAZ of steels B, H and J versus weld metal hardness. These values were determined at a punch speed of 133 mm/min.

Steel	Weld metal hardness (HV, 62.5kg)	FATT of HT HAZ (°C)
B	164	13
(4% ferrite in HT HAZ)	183	24
H	192	37
(32% ferrite in HT HAZ)	189	37
J	164	41
(48% ferrite in HT HAZ)	184	56

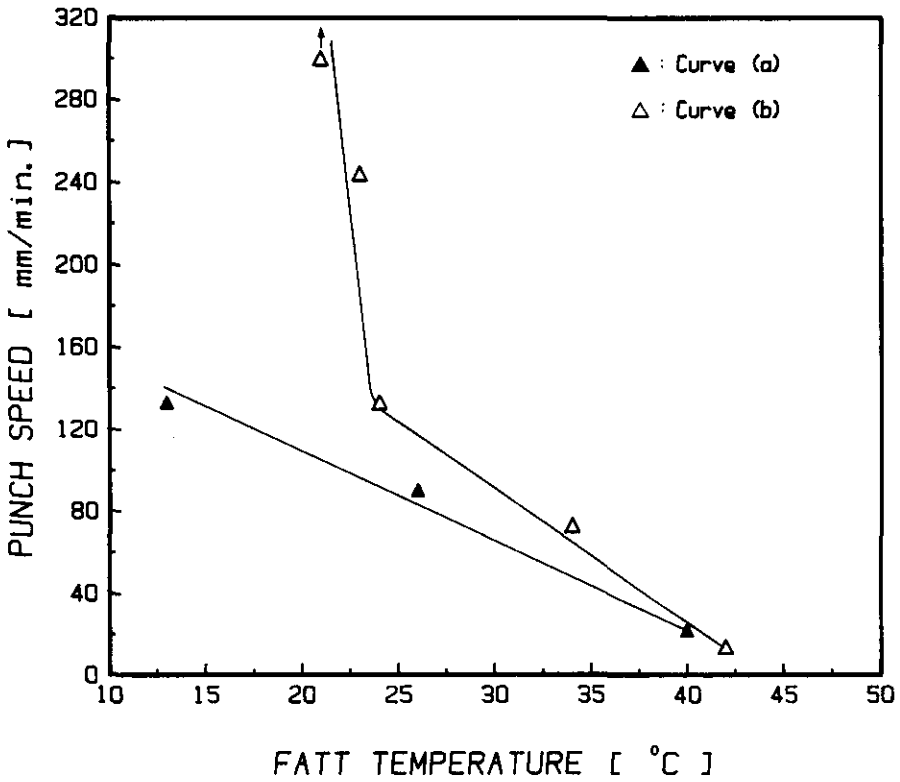

Figure 3.16: Punch speed for bend testing versus the FATT temperature of the HT HAZ of steel B.
Curve a: Weld metal hardness, 164 HV
Curve b: Weld metal hardness, 183 HV
(A FATT temperature of 21°C was obtained with impact loading in a Charpy impact machine)

4. DISCUSSION

The effects of the phase composition of the HT HAZ, of punch speed during bend testing, and of the weld metal mechanical properties on the fusion line fracture behaviour of bead-on-plate welds on 6 mm hot rolled 14% chromium steel plate may be explained by both Cottrell's and Davidenkov's flow stress-fracture stress theories.

In order to explain the experimental results by means of these theories the following assumptions have to be made:

a. The material at the notch tip (fig. 3.4) of a bead-on-plate bend specimen is modelled as a composite material consisting of the HT HAZ, the adjacent weld metal and fine grained HAZ.

b. The existance of a isostress field at the notch tip in the above-mentioned materials. The composite specimen at the notch tip is therefore assumed to be a series tensile specimen (fig. 3.17) with the composite materials in the specimen subjected to the same stress during bend testing or tensile loading.

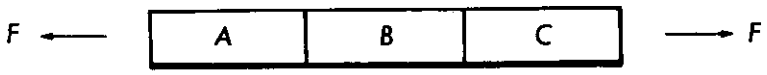

Figure 3.17: Series tensile composite specimen. The specimen consists of three different materials A, B and C.

4.1 Explanation of experimental results by means of the Cottrell-Petch fracture theory.

The Cottrell-Petch theory was discussed in detail in Chapter 2. Although this theory was originally developed for explaining only the ductile-brittle fracture mode transition in homogeneous materials, with decreasing temperature, grain size and loading rate, it may also be used to explain the fracture mode transition behaviour of a composite specimen, by superimposing the fracture stress and yield stress curves of the different

composite materials on the same figure. Since fracture was limited only to the weld metal adjacent to the fusion line and the HT HAZ of the 14% chromium steels in table 3.1, the curves for only the weld metal and HT HAZ of steel B, with 96% martensite in the HT HAZ, are superimposed on figure 3.18.

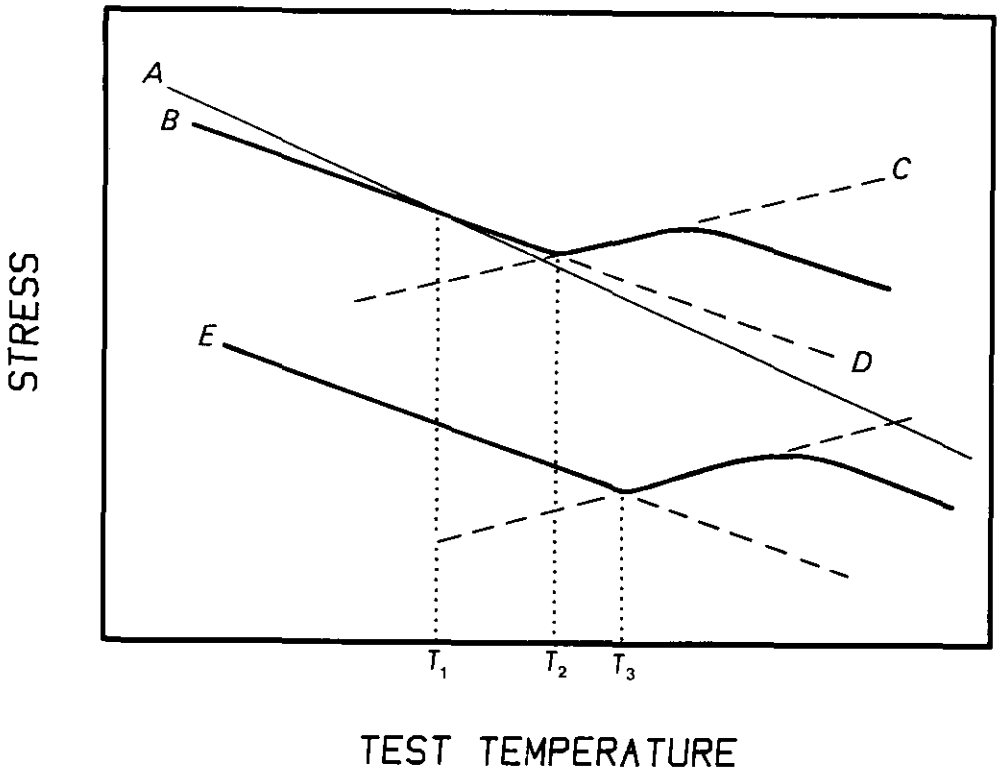

Figure 3.18: Fracture stress curves of the austenitic weld metal (A) and HT HAZ (B) of steel B with 96% martensite in the HT HAZ. The dotted curves C and D are respectively the theorectical fracture stress (σ_f according to Cottrell et al.) and yield stress (σ_{ys} according to Hall and Petch) curves of the HT HAZ. Curve E is the fracture stress curve for the HT HAZ of steel E with 79% ferrite in this zone.

Consider now only the fracture stress curve B for the HT HAZ. T_2 is then the true FATT temperature of this zone. At temperatures below and above T_2 the HT HAZ will fracture by respectively cleavage and ductile fracture at the fracture stresses indicated by curve B.

Only the ductile fracture stress curve A of the austenitic weld metal is indicated in figure 3.18 due to the fact that the FATT temperature of the

weld metal is much lower than that of the HT HAZ. The weld metal fracture stress curve A has a larger slope compared to the HT HAZ fracture stress curve B. This larger slope of curve A is derived from the fact that brittle cleavage fractures occurred in the HT HAZ at temperatures below the FATT temperature (lower HT HAZ fracture stress compared to the weld metal) while ductile fracture occurred in the weld metal adjacent to the fusion line at temperatures above the FATT temperature (lower weld metal fracture stress compared to HT HAZ).

The FATT temperature T_1 (fig. 3.18), which will be obtained for the composite specimen (this temperature is 13°C for steel B), is lower than the true FATT temperature T_2 for the HT HAZ.

The increase in the FATT temperature of the HT HAZ of e.g., steel B, from 13°C to 40°C (fig. 3.16) with a decrease in punch speed below 133 mm/min. may be explained as follows. With the much higher strain rate sensitivity of the yield strength and therefore the fracture strength of the BCC HT HAZ compared to the strain rate sensitivity of the FCC weld metal, the nett effect of a lower punch speed will be a displacement of the fracture stress curve B of the HT HAZ to lower stresses with the resultant intersection of curves A and B at the new FATT temperature which is higher than T_1 (fig. 3.18).

The increase in the FATT temperature of the HT HAZ of steel B from 13°C to 24°C with an increase in weld metal hardness from 164HV to 183HV may also be explained in a similar manner (table 3.3 and fig. 3.16). The fracture stress curve A of the weld metal in figure 3.18 is shifted to higher stresses with an increase in weld metal hardness with the intersection between curves A and B shifted to a higher FATT temperature.

Curve E in figure 3.18 represents the fracture stress curve for the HT HAZ of steel E with 79% ferrite in the HT HAZ. This curve is located at much lower stresses compared to curve B. This is due to the much larger grain size and lower martensite content of this zone compared to a zone with 96% martensite. The true FATT temperature T_3 of the HT HAZ with 79% ferrite may therefore be obtained since both the brittle and ductile fracture stresses are lower than the ductile fracture stress of the weld metal. Although curves B and E have the same slope, the slope of curve E may

actually be larger due to the larger grain size and smaller martensite content of the HT HAZ with 79% ferrite.

4.2 Explanation of experimental results by means of Davidenkov-Ludwik fracture theory

Although the Davidenkov-Ludwik fracture theory, which was discussed in chapter 2, was also originally developed for explaining the fracture mode transitional behaviour of notched tensile specimens, it may also be used to study the fracture behaviour of a series type composite specimen by superimposing the cleavage fracture stress, ductile fracture stress and flow stress curves of the different composite materials on the same figure.

Figure 3.19 shows such a superposition of the cleavage fracture- (curve A), ductile fracture- (curve B) and flow stress (curve D) curves of the HT HAZ of steel B with 96% martensite in this zone together with the ductile fracture- and flow stress curves of the weld metal. This figure applies to a test temperature of 13°C which is the FATT temperature of the HT HAZ of steel B at a punch speed of 133 mm/min. The curves in this figure therefore portrays the true stress-strain conditions at the notch tip of a bead-on-plate bend specimen which is being bent at a punch speed of 133 mm/min.

Consider now only the HT HAZ (curve D) and weld metal (curve E) flow stress curves. The yield strength of the HT HAZ at zero strain is much higher than that of the weld metal due to the high martensite content of this zone (fig. 3.15). The larger slope of curve E is due to the higher work hardening rate of the FCC austenitic weld metal.

Fracture will occur in the weld metal and/or HT HAZ when the flow stress curves intersect the fracture stress curves at $(\bar{\sigma}_2, \bar{\varepsilon}_2)$ and $(\bar{\sigma}_3\ \bar{\varepsilon}_3)$. With the present relative orientations of the curves in figure 3.19, the ductile weld metal fracture stress $\bar{\sigma}_2$ is less than the cleavage fracture stress $\bar{\sigma}_3$ of the HT HAZ. A ductile fracture will therefore initiate in the weld metal adjacent to the fusion line during bend testing. As the ductile crack propagates in the weld metal adjacent to the fusion line (it was found to propagate at a distance of 0.2-0.3 mm from the fusion line) the HT HAZ is subjected to increasingly higher stresses due to the

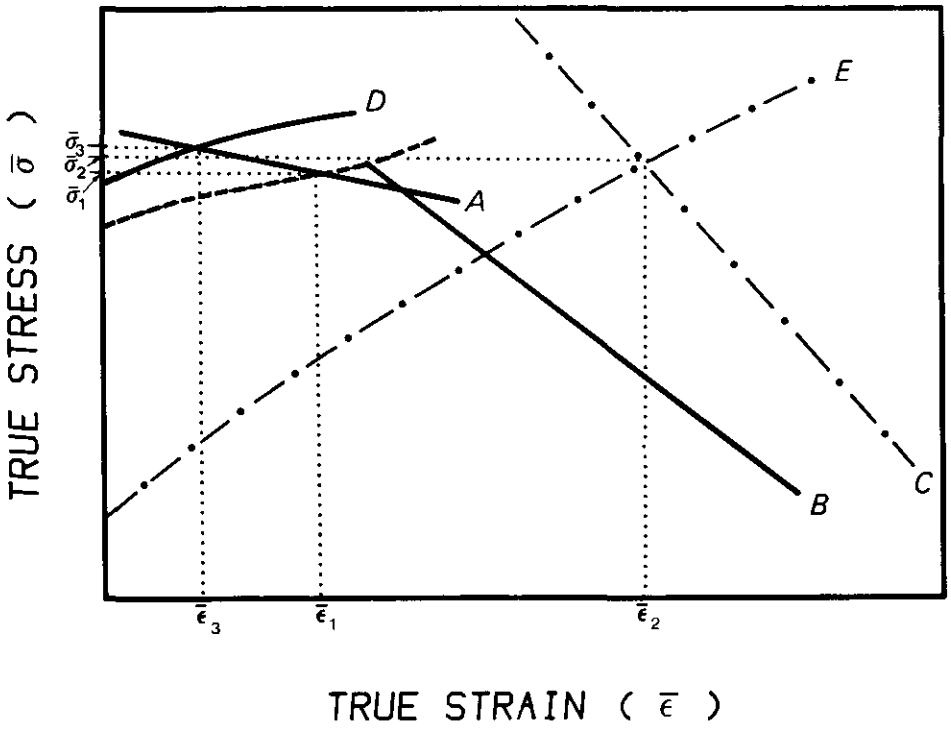

Figure 3.19: Fracture stress and flow stress curves for the weld metal and HT HAZ of steel B with 96% martensite in the HT HAZ. The curves describe the true stress-strain conditions at the notch tip of a bead-on-plate bend specimen which is being tested at 13°C at a punch speed of 133 mm/min.
Curve A : Cleavage fracture stress for the HT HAZ
Curve B : Ductile fracture stress for the HT HAZ
Curve C : Ductile fracture stress for the 316L weld metal
Curve D : Flow stress curve for the HT HAZ
Curve E : Flow stress curve for the 316L weld metal

fact that the fusion line is not oriented normal to the plate surface. The isostress conditions which were assumed originally are actually only valid as far as the fusion line notch tip fracture behaviour is concerned. Cleavage fracture initiation may therefore occur in the HT HAZ, after a ductile crack has propagated for a certain distance in the weld metal, when the cleavage fracture stress $\bar{\sigma}_3$ of this zone is exceeded. Bead-

on-plate bend specimens of steel B fractured in this manner at a FATT temperature of 13°C.

When the abovementioned bend specimens were tested at a lower punch speed of 10 mm/min., a cleavage crack initiated and propagated in the HT HAZ. This fracture made transition may be explained by the much higher strain rate sensitivity of the BCC HT HAZ. The nett effect of the lower punch speed is therefore a displacement of the flow stress and fracture stress curves of the HT HAZ to lower stresses relative to the curves for the weld metal. This displacement may be simplified by a shift of curve D to lower stress (dotted curve in fig. 3.19) with the cleavage fracture stress $\bar{\sigma}_1$, of the HT HAZ now lower than the ductile fracture stress $\bar{\sigma}_2$ of the weld metal. HT HAZ cleavage fracture initiation may also be caused by an increase of the weld metal strength and therefore an increase in weld metal fracture stress.

The notch tip true stress-strain conditions at the FATT temperature of 74°C for the HT HAZ of a bend-on-plate bend specimen of steel E with 79% ferrite in the HT HAZ is portrayed by the fracture and flow stress curves in figure 3.20.

The flow stress and fracture stress curves for the HT HAZ of steel E in figure 3.20 are located at lower stresses compared to the respective curves (dotted curves) for this zone with 96% martensite (fig. 3.19). This is due to the larger grain size and lower martensite content (fig. 3.1). Cleavage and ductile fractures will occur in the HT HAZ at stresses which are represented by the intersection of curve D with respectively curves A and B. A ductile weld metal fracture will occur at the intersection of curves E and C. Since the ductile fracture stress of the weld metal $\bar{\sigma}_1$ is much higher than both the cleavage and ductile fracture stresses of the HT HAZ, the true FATT temperature of the HT HAZ may therefore be determined. At temperatures lower than 74°C, curves A, B and D are shifted to higher stresses relative to curves C and E with the flow stress curve D intersecting the cleavage fracture stress curve A; a cleavage fracture will occur therefore in the HT HAZ. At temperatures above 74°C, curves A, B and D will be shifted to lower stresses relative to curves C and E with the flow stress curve D intersecting the ductile fracture stress curve B; a ductile fracture will occur therefore in the HT HAZ.

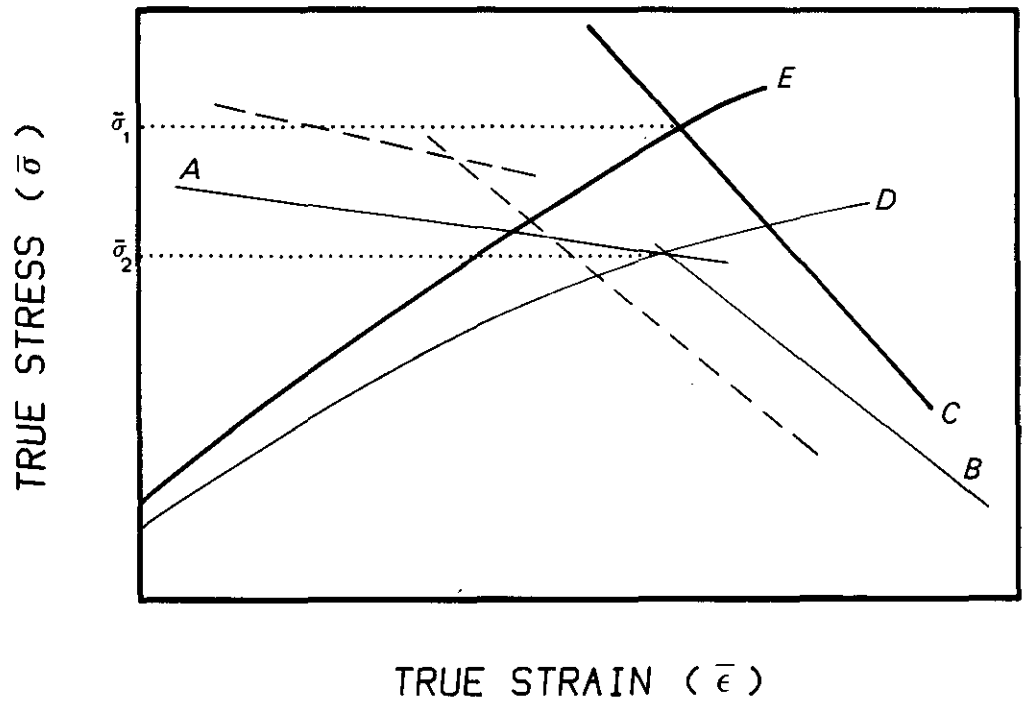

Figure 3.20: Fracture stress and flow stress curves for the weld metal and HT HAZ of steel E with 79% ferrite in the HT HAZ. The curves describe the true stress-strain conditions at the notch tip of a bead-on-plate bend specimen which is being tested at 74°C at a punch speed of 133 mm/min.
Curve A : Cleavage fracture stress for the HT HAZ
Curve B : Ductile fracture stress for the HT HAZ
Curve C : Ductile fracture stress for the 316L weld metal
Curve D : Flow stress curve for the HT HAZ
Curve E : Flow stress curve for the 316L weld metal
The dotted curves are the cleavage and ductile fracture stress curves for a HT HAZ with 96% martensite in this zone (fig. 3.19).

The fact that fracture was limited to only the weld metal adjacent to the fusion line and the HT HAZ, implies that both the cleavage and ductile fracture stresses of the fine grained HAZ are much higher than the corresponding stresses of both the weld metal and HT HAZ even with 96% martensite in the HT HAZ.

With reference to the explanations for the fusion line fracture behaviour of bead-on-plate AISI 316L welds on 6 mm hot rolled 14% chromium steel

plate in terms of Cottrell's and Davidenkov's flow stress-fracture stress theories, it may be concluded that the fusion line fracture behaviour is determined by the following factors:

a. Relative weld metal and HT HAZ mechanical properties: yield strength, work hardening rate, cleavage and ductile fracture stresses.

b. Relative strain rate sensitivities of the yield and fracture strength of the weld metal and HT HAZ.

c. Mechanical properties of the fine grained HAZ and base metal.

d. Fusion line orientation relative to the plate surface.

4.3 High temperature HAZ fracture toughness

The HT HAZ FATT temperatures which were obtained at punch speeds of respectively 10 mm/min. and 133 mm/min. for the 14% chromium steels in table 3.1 are summarized in figure 3.21. Superimposed on this figure are suggested curves for the minimum FATT temperatures of the HT HAZ (for a punch speed of 10 mm/min) for, respectively, the titanium and vanadium stabilised steels.

Curve B shows that the FATT temperatures of the HT HAZ of the titanium stabilised steels decreased by less than 32°C (from 74°C to 42°C) by an increase in the martensite content from 21% to 96% in the HT HAZ. These very high FATT temperatures of the HT HAZ, which are expected to be higher with impact loading, indicates that the fracture toughness of the HT HAZ of welds on 6 mm hot rolled 14% chromium steel plate is relatively low. Furthermore, the fact that the fracture toughness of this HT HAZ is not improved significantly by large fractions low carbon, titanium stabilised, grain boundary martensite, indicates that the fracture toughness is determined by another important factor or phenomenon which has not yet been identified. There is therefore no sense in substituting some of the titanium in the steel with vanadium as stabilising element, in order to limit the amount of coarse segregated titanium carbonitrides at the plate centre, since even the fracture toughness of the HT HAZ of steels stabilised with titanium only is unacceptably low.

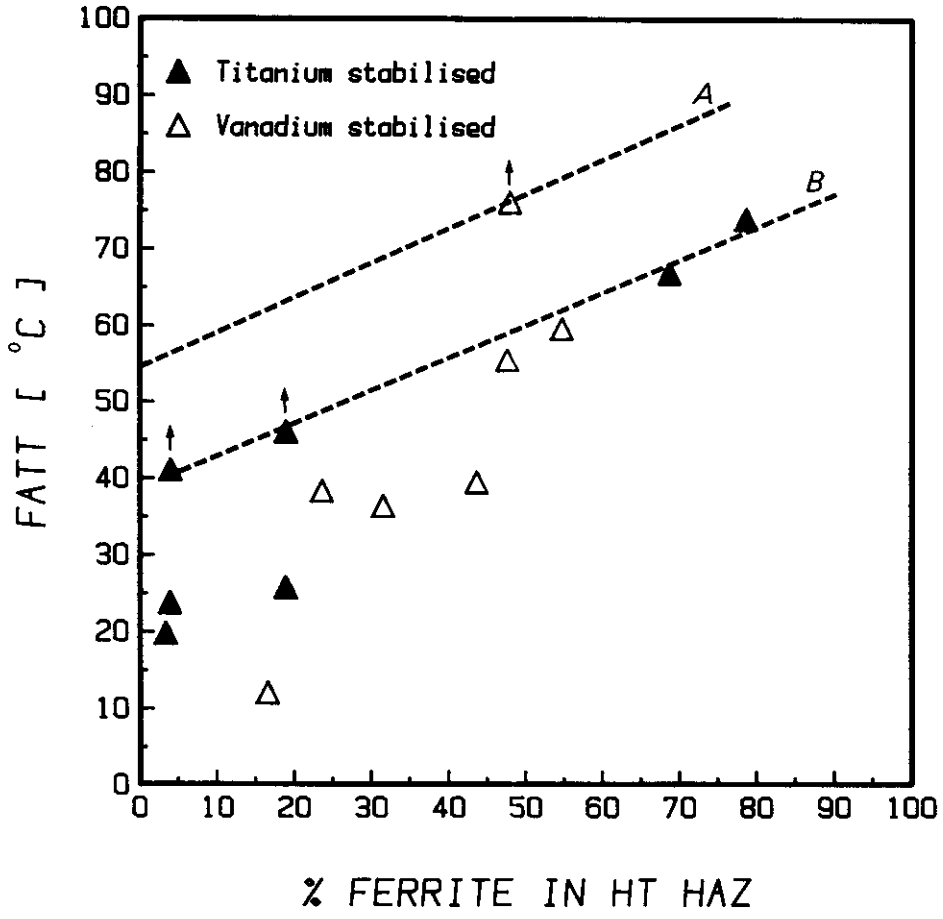

Figure 3.21: FATT temperature versus the ferrite content of the HT HAZ of bead-on-plate 316L welds on 6 mm hot rolled 14% chromium steel plate. The values indicated by arrows were obtained at a punch speed of 10 mm/min. with the other values obtained at a punch speed of 133 mm/min. (The fusion line orientation relative to the plate surface of the bead-on-plate specimens ranged from 120° to 124°)

Curve A: Minimum suggested FATT temperatures for the HT HAZ of vanadium stabilised 14% chromium steels

Curve B: Minimum suggested FATT temperatures for the HT HAZ of titanium stabilised 14% chromium steels

It may therefore be concluded that although the new notch-toughness test has certain practical limitations, valuable information has been obtained on the influence of the narrow coarse grained HT HAZ on the notch-toughness of welds on 6 mm 14% chromium steel plate. Due to the low fracture toughness of the HT HAZ, 14% chromium steel plate is not recommended for any structural applications. Brittle fracture may occur in welded

structures, especially in the as-welded condition, when high tensile residual stresses are present together with inevitable fusion line defects such as undercutting, lack of side-wall fusion, incomplete penetration and slag inclusions. In critrical applications, when a triaxial stress state develops in weld configurations offering a high degree of constraint the material is particulary susceptable to brittle fracture.

5. SUMMARY

a. A new test method has been developed which gives a reasonable indication of the influence of the narrow, coarse grained high temperature weld HAZ on the fusion line notch-toughness of bead-on-plate AISI 316L welds on respectively 6 mm hot rolled titanium and vanadium stabilised 14% chromium steels.

b. The FATT temperature of the HT HAZ of steels, with less than 60 percent ferrite in the HT HAZ, increased with decreasing punch speeds (during slow three point bend testing) below 133 mm/min. This phenomenon is explained in terms of Cottrell's and Davidenkov's fracture theories and the relative strain rate sensitivities of the yield and fracture strengths of the FCC austenitic weld metal and BCC HT HAZ.

c. The FATT temperatures increased with higher weld metal mechanical properties.

d. The actual or true FATT temperatures of the HT HAZ, for slow bend testing, of the two titanium stabilised steels with 69% and 79% ferrite in the HT HAZ, is 67°C and 74°C, respectively. The actual HT HAZ FATT temperatures of both the titanium and vanadium stabilised steels with less than 60% ferrite in the HT HAZ, are higher than the reported values. This is due to the fact that the fusion line notch-toughness of welds is enhanced by the ductile properties of the austenitic weld metal.

e. The HT HAZ FATT temperatures of the titanium stabilised steels are reduced by less than 32°C, during slow bend testing, as a result of an increase in martensite content from 21% to 96%. The HT

HAZ FATT temperatures of the vanadium stabilised steels are higher than that for the titanium stabilised steels.

f. It is concluded that the HT HAZ fracture toughness of 14% chromium steels is relatively low, even with high percentages of low carbon martensite.